

Broad-line and Multi-wave Band Emission from Blazars

T. F. Yi,¹ G. Z. Xie,^{2,3†}

¹*Physics Department, Yunnan University, Kunming 650091, P. R. China*

²*National Astronomical Observatories/Yunnan Observatory, Chinese Academy of Sciences, P. O. Box 110, Kunming 650011, P. R. China*

³*Yunnan Astrophysics Center, Yunnan University, Kunming 650091, P. R. China*

[†]*send offprint requests to G. Z. Xie; Email:gzxie@public.km.yn.cn*

(Received <reception date>; accepted <acceptation date>)

Abstract

We study the correlations of the flux of the broad-line emission (F_{BLR}) with the X-ray emission flux, optical emission flux at 5500 Å and radio emission flux at 5 GHz, respectively, for a large sample of 50 Blazars (39 flat-spectrum radio quasars (FSRQs) and 11 BL Lac objects). Our main results are as follows. There are very strong correlations between F_{BLR} and F_X and between L_{BLR} and L_X in both states for 39 FSRQs and the slopes of the linear regression equations are almost equal to 1. There are weak correlations between F_{BLR} and F_X and between L_{BLR} and L_X for 11 BL Lac objects in both states, and the slopes of the linear regression equations are close to 1. There are significant correlations between F_{BLR} and F_X and between L_{BLR} and L_X for 50 blazars in both states, the slopes of both the linear regression equations are also close to 1. These results support a close link between relativistic jets and accretion on to the central Kerr black hole. On the other hand, we find that BL Lac objects have low accretion efficiency η , whereas FSRQs have high accretion efficiency η . The unified model of FSRQs and BL Lac objects is also discussed.

Key words: galaxies: accretion disks—BL Lacertae objects: general—galaxies: jets—quasars: emission lines

1. Introduction

The relation between jets and accretion processes in active galactic nuclei (AGN) is one of the most fundamental and open problems. In current theoretical models of the formation of the jet, the power is through accretion and then extracted from the disk/black hole spin energy and converted in the kinetic power of the jet (Blandford & Znajek 1977; Blandford & Payne 1982; Maraschi & Tavecchio 2003). In both cases the magnetic field play a major role in channelling power from the black hole spin or disk into the jet, in both scenarios it should be sustained by matter accreting onto the black hole, leading one to expect a relation between accretion power and jet power (Maraschi et

al. 2003; Xie et al. 2007). Recently, the concept of jet-disk symbiosis was introduced (Cao & Jiang 1999). The relativistic jet model plus mass and energy conservation in the jet-disk system was applied to study the relation between disk and jet luminosities (Cao & Jiang 1999; Falcke & Biermann 1995; Falcke, Malkan & Biemann 1995). An effective approach to explore the link between the mentioned above two phenomena is to study the relation between broad-line emission luminosity and jet power at different wavelength (Dai et al. 2007; Cao & Jiang 1999; Maraschi & Tavecchio 2003; Celotti, Padovani & Ghisellini 1997; Serjeant et al. 1998; Xu et al. 1999; Xie et al. 2007). Celotti, Padovani & Ghisellini (1997) considered a large sample of radio-loud objects, and derived the accretion luminosity from the Broad emission lines when available. They explored the relation between the disk and jet using the correlation between the broad-line luminosity and kinetic power. The kinetic power of jets can be estimated by using the direct radio emission data of the jets close the nucleus, as resolved by very-long-baseline interferometry (VLBI) and the standard synchrotron self-Compton theory of Celotti & Fabian (1993). They found evidence for a link between jets and disks, although the statistical significance was too low to draw a firm conclusion.

Cao & Jiang (1999) found a significant correlation between radio and broad-line emission for a sample of radio-loud quasars that supports a close link between accretion processes and relativistic jets. It is well known that blazars are in fact the best laboratories to study the physics of relativistic jets. For a small sample of blazars, Maraschi & Tavecchio (2003) also found a significant correlation between the luminosity carried by relativistic jets and the nuclear luminosity provided by accretion, using the good-quality broadband X-ray data provided by the BeppoSAX satellite. Their results also support a close accretion on to a rapidly spinning central black hole. However, in a flux-limited sample that covers a wide range of redshift, a correlation can appear in luminosity even though there is no intrinsic correlation in the sources because the luminosity is strongly correlated with redshift (Mücke et al. 1997). In order to avoid the redshift bias to data, in this paper we will discuss correlations between flux densities (and the corresponding luminosities) in different wave bands because they are less susceptible to such distortions.

In this paper, for a large sample of blazars, we study the correlations of the broad-line flux with X-ray flux, optical flux and radio flux, respectively, and the correlations of the broad-line luminosity with X-ray luminosity, optical luminosity and radio luminosity, respectively. The cosmological parameters $H_0 = 75 \text{ km s}^{-1} \text{ Mpc}^{-1}$ and $q_0 = 0.5$ have been adopted in this work.

2. Sample Description

Based on the catalogue of blazars compiled by Donato et al. (2001) and the catalogue of the broad emission line information of radio-loud sources compiled by Cao & Jiang (1999), we compiled a sample of 50 blazars, for which the total broad-line flux ($\text{erg cm}^{-2}\text{s}^{-1}$), X-ray flux at 1 keV in μJy , optical flux at 5500 Å and radio flux at 5 GHz given by Cao & Jiang (1999) and Donato et al. (2001) are available. The relevant data for 50 blazars are listed in Table 1. The columns in this table are as follows: Column (1): name of the source (IAU); column (2): redshift; column (3): radio flux (F_R) at

5 GHz in Jy; column (4): V band optical flux (F_O) in millijanskys (mJy); column (5): 1 keV X-ray flux (F_X) in microjanskys (μ Jy), the first entry is for the high state, the second for the low state; column (6): X-ray photon spectral index; column (7): estimated total broad-line flux ($\text{erg cm}^{-2}\text{s}^{-1}$); Column (8): the class. In Table 1, the data of X-ray, optical and radio bands are taken from the catalogue compiled by Donato et al. (2001), and the data of the broad-line emission are taken from the catalogue compiled by Cao & Jiang (1999). In table 1, for the X-ray band, all 50 blazars have fluxes, but only 26 of them have fluxes in both high and low states. For the remaining 24 objects, we can not be certain whether they are in a high state or low state. In the following analysis, we will consider two possible cases: (1) assuming them to be in a high state, and (2) assuming them to be a low state.

3. Correlation Analysis of Fluxes and Luminosities between Various Wave Bands

Radio, optical and X-ray flux densities are K-corrected according to $F_\nu = F_\nu^{ob}(1+z)^{\alpha-1}$ and $\alpha_R = 0.0$, $\alpha_O = 1.0$, $\alpha_X = \alpha_X^{ph} - 1$ (Comastri et al. 1997). The X-ray photo spectral index α_X^{ph} has been given by Donato et al. (2001) and listed in column (6) of Table 1. Linear regression is applied to the relevant data to analyze the correlations of flux densities and luminosities between different wave bands. The analysis results are given in Table 2. The principal results of Table 2 are as follows:

(1) There is strong correlation between $\log F_{BLR}$ and $\log \nu F_X$ in high state for 50 blazars (Fig. 1 and Table 2). The linear regression equation in high state is

$$\log F_{BLR} = 0.98 \log \nu F_X - 0.83, \quad (1)$$

with correlation coefficient $r = 0.64$ and chance probability $p < 10^{-4}$. The slope of the linear regression equation is almost equal to 1. In Fig. 1, the solid line is the regression line of all 50 blazars.

(2) From Table 2, one can see that there is very strong correlations between $\log F_{BLR}$ and $\log \nu F_X$ in high state for 39 FSRQs. The linear regression equation in high state is

$$\log F_{BLR} = 1.00 \log \nu F_X - 0.43, \quad (2)$$

with $r = 0.76$ and $p < 10^{-4}$. The result is also plotted in Fig. 1. The dash line is the linear regression equation (2). In addition, one notes that the slop of the equation (2) is almost equal to 1.

(3) There are weak correlations between $\log F_{BLR}$ and $\log \nu F_X$ in both states for 11 BL Lac objects only (Table 2). However, one can see that the slope of the linear regression equation in high state is close to 1 (Table 2). The linear regression equation in high state is

$$\log F_{BLR} = 0.74 \log \nu F_X - 4.59, \quad (3)$$

with $r = 0.65$ and $p = 3.1 \times 10^{-2}$. The result is also plotted in Fig. 1. The dot line is the regression line of the BL Lac objects.

(4) A strong correlation ($r = 0.67$, $p < 10^{-4}$) between $\log F_{BLR}$ and $\log \nu F_X$ in low state has been found when both FSRQs and BL Lac objects are considered (50 blazars). The correlation is , however, much strong considering FSRQs only ($r = 0.63$, $p < 10^{-4}$) and is weak for BL Lac objects only ($r = 0.72$,

$p = 1.2 \times 10^{-2}$). The results are shown in Fig. 2. In Fig. 2, the solid line is the regression line of all 50 blazars, the dash line and dot line are the regression lines of FSRQs and BL Lac objects, respectively. From Table 2, one can see that the slopes of the linear regression equations in low state are close to 1 in all cases.

(5) A significant correlation ($r = 0.63$, $p < 10^{-4}$) between $\log F_{BLR}$ and $\log \nu F_O$ has been found when both FSRQs and BL Lac objects are considered (50 blazars) (see Fig. 3). The correlation is, however, very strong considering FSRQs only ($r = 0.71$, $p < 10^{-4}$) and is weak for BL Lac objects only ($r = 0.68$, $p = 2.2 \times 10^{-2}$). However, from Table 2 one can see that the slopes of the linear regression equations in optical band are close to 1 in all cases.

(6) A significant correlation ($r = 0.43$, $p = 1.9 \times 10^{-3}$) between $\log F_{BLR}$ and $\log \nu F_R$ has been found when both FSRQs and BL Lacs are considered (see Fig. 4). The correlation is, however, very strong considering FSRQs only ($r = 0.54$, $p \approx 10^{-4}$) and not for BL Lac objects only ($r = 0.49$, $p = 1.3 \times 10^{-1}$).

(7) A correlation between $\log L_X$ and $\log L_{BLR}$ for 50 blazars in high state (see Fig. 5) is also significant. The correlation coefficient is $r = 0.78$ and the chance probability is $p < 10^{-4}$. The linear regression equation is

$$\log L_{BLR} = 1.23 \log L_X - 11.12. \quad (4)$$

The slope of the linear regression equation (4) is close to 1.

(8) There is a very strong correlation between $\log L_X$ and $\log L_{BLR}$ for 39 FSRQs in high state. The correlation coefficient is $r = 0.84$ and a chance probability is $p < 10^{-4}$. The linear regression equation is

$$\log L_{BLR} = 1.12 \log L_X - 5.62. \quad (5)$$

The slope of the linear regression equation (5) is very close to 1.

(9) There is a weak correlation between $\log L_X$ and $\log L_{BLR}$ for 11 BL Lac objects in high state. The correlation coefficient $r = 0.73$ and the chance probability is $p = 1.0 \times 10^{-2}$. The linear regression equation is

$$\log L_{BLR} = 0.77 \log L_X + 8.95. \quad (6)$$

The slope of the linear regression equation (6) is also close to 1.

(10) A strong correlation ($r = 0.81$, $p < 10^{-4}$) between $\log L_X$ and $\log L_{BLR}$ in low state has been found for 50 blazars. The correlations are significant for FSRQs only ($r = 0.74$, $p < 10^{-4}$) and for BL Lac objects only ($r = 0.79$, $p = 3.8 \times 10^{-3}$). As shown in Fig. 6, the solid line is the regression line of all 50 blazars, and the dash line and dot line are the regression lines of FSRQs and BL Lac objects, respectively. In Table 2, We can see that the slopes of the linear regression equations in low state are close to 1 in all cases.

(11) There are also strong correlations between $\log L_O$ and $\log L_{BLR}$, and between $\log L_R$ and $\log L_{BLR}$, as shown in Fig. 7 and 8, respectively. The slopes are also close to 1 in all cases.

4. The Jet-Disk Relationship

According to Ghisellini (2006), if relativistic jets are powered (at least initially) by a Poynting flux, one can derive a simple expression for the maximum value of their power, under some reasonable assumptions. The Blandford & Znajek (1977) power can be written as:

$$L_{BZ} \sim 6 \times 10^{20} \left(\frac{a}{m}\right)^2 \left(\frac{M_{BH}}{M_\odot}\right)^2 B^2 \text{ erg s}^{-1}, \quad (7)$$

where L_{BZ} is the luminosity, M_{BH} is the mass of black hole, M_\odot is the solar mass, $\frac{a}{m}$ is the specific black hole angular momentum (~ 1 for maximally rotating black holes), and B is the magnetic strength in units of Gauss. Assuming that the value of magnetic energy density $U_B \equiv \frac{B^2}{8\pi}$ close to black hole is a fraction ε_B of the available gravitational energy:

$$U_B = \varepsilon_B \frac{GM_{BH}\rho}{R} = \varepsilon_B \frac{R_S}{2R} \rho c^2, \quad (8)$$

where $R_S = \frac{2GM_{BH}}{c^2}$ is the Schwarzschild radius. Based on the accretion disk theory the mass density ρ is linked to the accretion rate \dot{M} through

$$\dot{M} = 2\pi R H \rho \beta_r c, \quad (9)$$

where $\beta_r c$ is the radial in falling velocity, H is the disk thickness. As in stars, the fundamental process at work in an active nucleus is the conversion of mass to energy. This is done with some efficiency η , the mass accretion rate $\dot{M} = \frac{dM}{dt}$ is linked to the observed luminosity produced by the accretion disk

$$L_{disk} = \eta \dot{M} c^2. \quad (10)$$

From equations (7), (8), (9), (10), the Blandford-Znajek jet power can be written as :

$$L_{BZ,jet} \sim \left(\frac{a}{m}\right)^2 \frac{R_S^3}{H R^2} \frac{\varepsilon_B}{\eta} \frac{L_{disk}}{\beta_r}. \quad (11)$$

The maximum jet power can be written as (Ghisellini 2006):

$$L_{jet} \sim \frac{L_{disk}}{\eta}. \quad (12)$$

In addition, on the basis of present theories of accretion disk, the broad-line region (BLR) is photoionized by a nuclear source (probably radiation from the disk), Maraschi & Tavecchio (2003) obtained

$$L_{BLR} = \tau L_{disk}, \quad (13)$$

where τ represents the fraction of the central emission reprocessed by the BLR, usually assumed to be 0.1. From equation (12) and (13), we have

$$L_{BLR} = \tau \eta L_{jet}. \quad (14)$$

It is well known that according to the accretion disk theory, η is not a constant. It ranges from 0.057 to 0.42. However in our previous works (Xie et al. 2002; 2003), one prove that the central black hole of blazars are probably Kerr black holes. Its range should be narrow (Xie et al. 2005). From equation (14), we can have

$$\log L_{BLR} = \log L_{jet} + \log \eta + const. \quad (15)$$

From the equation (15), we can see that the theoretical predictions are as follows. (1) The slope of $\log L_{BLR}$ - $\log L_{jet}$ linear relation should be 1. η is an important physical parameter. (2) Since η is not the same for all objects, $\log \eta$ will contribute to the dispersion around the linear relation.

5. Discussions and Conclusions

From Fig. 1 to Fig. 8 and Table 2, we can see that the straight lines of linear regression equations of BL Lac parallel almost the straight line of linear regression equations of FSRQs in X-ray, optical and radio bands, respectively. However BL Lac objects systematically lie somewhat below the FSRQs. On the other hand it is worth noting that there is very strong correlation between F_{BLR} and F_X in both states for all 50 Blazars, and there are also significant correlations between F_{BLR} and F_O , and between F_{BLR} and F_R . In addition, the slopes of the straight lines of all linear regression equations of blazars in X-ray, optical and radio bands are also close to 1. On the basis of the theoretical results of equation (15) and the empirical results mentioned above, we seem to obtain following implications. (1) The coupling between the jet and accretion disk of blazars is very close, leading to the fact that F_{BLR} correlate significantly with multi-wave band fluxes. (2) BL Lac objects are a subclass of blazars which have low accretion coefficient η . (3) FSRQs are also a subclass of blazars which have high accretion coefficient η . (4) These results seem to show that FSRQs and BL Lac objects should be regarded as a class which shows blazar behavior (Xie et al. 2004; 2006). (5) The correlation between disk and jet emission does not depend on the emission state of the AGN. The idea of the unification of FSRQs and BL Lac objects is confirmed by a new independent evidence. It is very interesting to note that if we compare our results with the theoretical models of Ghisellini (2006) and Maraschi & Tavecchio (2003). We can see that our experimental results are consistent with the theoretical prediction of equation (15) in section 5 of this paper, this is, these results mentioned above (both the experimental and the theoretical) suggest a close link between the formation of relativistic jet and accretion on to the central Kerr black hole. Thus, we provide a solid basis for these theoretical speculations of Ghisellini (2006) and Maraschi & Tavecchio (2003).

From Table 2, one can see that there are very strong correlations between F_X and F_{BLR} or between F_O and F_{BLR} in all cases. However, there is a significant correlation between F_R and F_{BLR} for all blazars or for FSRQs, and there is weak correlation between F_R and F_{BLR} for BL Lac objects. These experimental results support the theory that the optical-UV and X-ray emission is energizing the emission of the broad-line region, so the more optical-UV and X-rays emission in the core, the more broad-line region emission. It is true that in blazars the jet emission is highly beamed, so it is possible that much of the emission of the observed X-ray flux may be from the jet (although even in the brightest objects, the X-ray flux densities are much weaker than the core). Even if the jet synchrotron emission does dominate in the X-ray, to be called an FSRQ the broad-line region emission must be commensurately bright enough to be seen over the synchrotron continuum, thereby introducing these

correlations. This might explain why the correlations obtained in this paper are weaker for BL Lac objects (because BL Lac objects have no blue bump). In addition, the radio flux depends almost exclusively on the parameters of a beamed jet, whereas the optical-UV and X-ray flux depends on both the unbeamed accretion disk and the beamed jet; and the broad-line region flux depend on an unbeamed accretion disk. Therefore, these results lead us to obtain that a strong correlation between F_X and F_{BLR} or between F_O and F_{BLR} , and a significant correlation between F_R and F_{BLR} , which based on the theoretical model of the formation of the jet. It is these correlations and difference of the correlations that imply a close link between accretion disks and jets (i.e. jet-disk symbiosis).

The authors would like to thank the referee Elena Pian for her helpful suggestions and comments.

References

- Blandford, R. D., & Payne, D. G. 1982, MNRAS, 199, 883
 Blandford, R. D., & Znajek, R. L. 1977, MNRAS, 179, 433
 Cao, X. W., & Jiang, D. R. 1999, MNRAS, 307, 802
 Celotti, A., & Fabian, A. C. 1993, MNRAS, 264, 228
 Celotti, A., Padovani, P., & Ghisellini, G. 1997, MNRAS, 286, 415
 Comastri, A., Fossati, G., Ghisellini, G., & Molendi, S. 1997, ApJ, 480, 534
 Dai, H., Xie, G. Z., Zhou, S. B., Li, H. Z., Chen, L. E., & Ma, L. 2007, AJ, 133, 2187
 Donato, D., Ghisellini, G., Tagliaferri, G., & Fossati, G. 2001, A&A, 375, 739
 Falcke, H., & Biermann, P. L. 1995, A&A, 293, 665
 Falcke, H., Malkan, M. A., & Biermann, P. L. 1995, A&A, 298, 375
 Ghisellini, G. 2006, astro-ph/0611077, Proceeding of Science, VI Microquasar workshop: Microquasars beyond, September, 18-22, 2006, Societa del Casino, Como, Italy
 Maraschi, L., & Tavecchio, F. 2003, ApJ, 593, 667
 Mücke, A., et al. 1997, A&A, 320, 33
 Serjeant, S., Rawlings, S., & Maddox, S. J. 1998, MNRAS, 294, 494
 Xie, G. Z., Dai, H., & Zhou, S. B. 2007, AJ, 134, 1464
 Xie, G. Z., Liang, E. W., Xie, Z. H., & Dai, B. Z. 2002, AJ, 123, 2352
 Xie, G. Z., Ma, L., Liang, E. W., Chen, L. E., Zhou, S. B., & Xie, Z. H. 2003, AJ, 126, 2108
 Xie, G. Z., Chen, L. E., Li, H. Z., Mao, L. S., Dai, H., Xie, Z. H., Ma, L., & Zhou, S. B. 2005, ChJAA, 5, 463
 Xie, G. Z., Dai, H., Mao, L. S., Li, H. Z., Liu, H. T., Zhou, S. B., Ma, L., & Chen, L. E. 2006, AJ, 131, 1210
 Xie, G. Z., Zhou, S. B., Liu, H. T., Chen, L. E., & Ma, L. 2004, IJMPD, 13, 347
 Xu, C., Livio, M., & Baun, S. 1999, AJ, 118, 1169

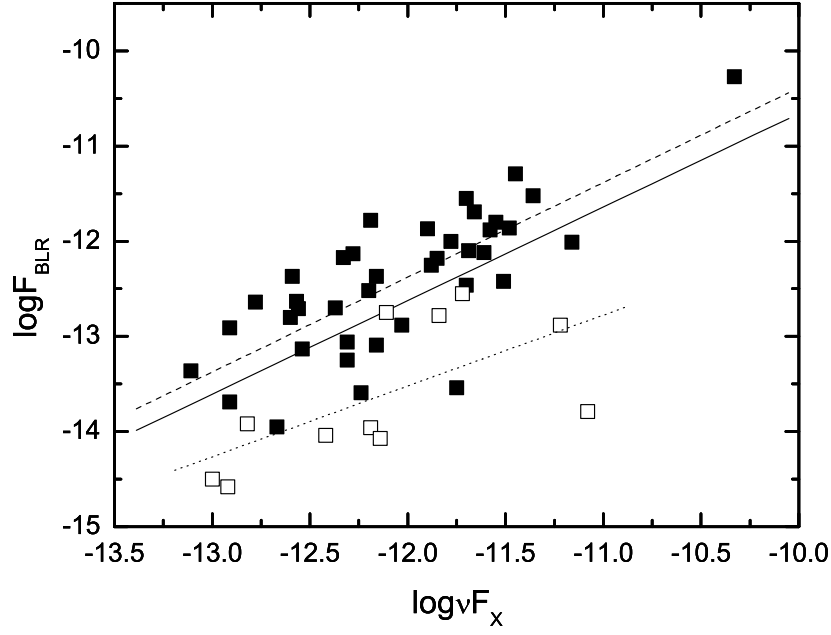


Fig. 1. Correlation between $\log \nu F_X$ and $\log F_{BLR}$ in high state for 50 blazars. The filled squares indicate 39 FSRQs, and the open squares indicate the 11 BL Lacs. The solid line is the regression line of all 50 blazars ($k = 0.98$, $r = 0.64$ and $p < 10^{-4}$), the dash line and dot line are the regression lines of FSRQs ($k = 1.00$, $r = 0.76$ and $p < 10^{-4}$) and BL Lacs ($k = 0.74$, $r = 0.65$ and $p = 3.1 \times 10^{-2}$), respectively.

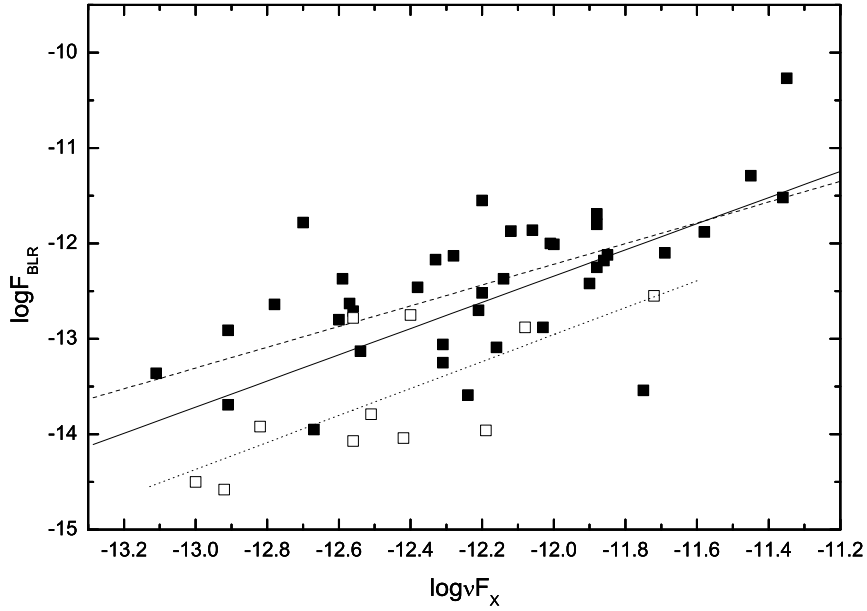


Fig. 2. Correlation between $\log \nu F_X$ and $\log F_{BLR}$ in low state for 50 blazars. The filled squares indicate 39 FSRQs, and the open squares indicate the 11 BL Lacs. The solid line is the regression line of all 50 blazars ($k = 1.37$, $r = 0.67$ and $p < 10^{-4}$), the dash line and dot line are the regression lines of FSRQs ($k = 1.09$, $r = 0.63$ and $p < 10^{-4}$) and BL Lacs ($k = 1.41$, $r = 0.72$ and $p = 1.2 \times 10^{-2}$), respectively.

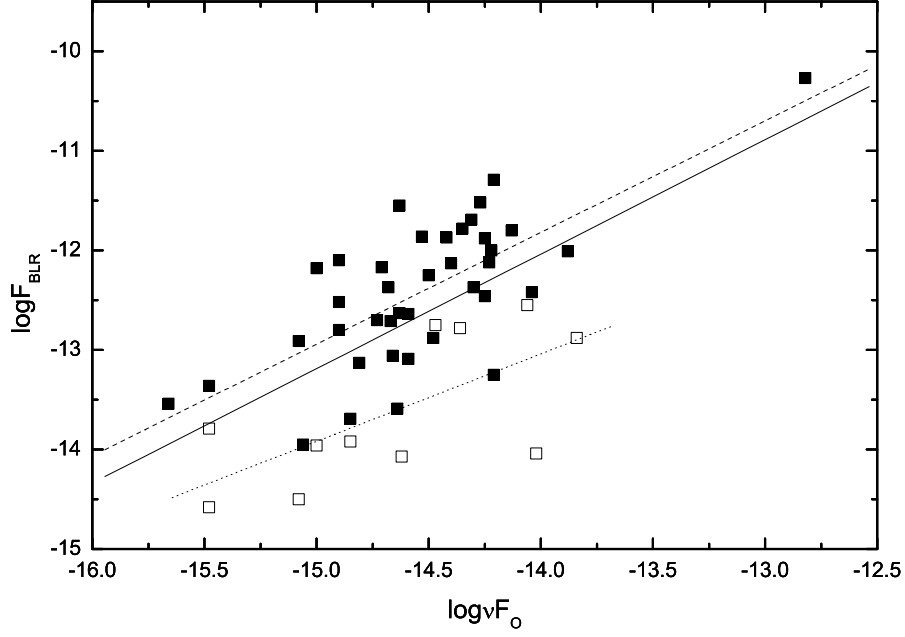


Fig. 3. Correlation between $\log \nu F_O$ and $\log F_{BLR}$ for 50 blazars. The filled squares indicate 39 FSRQs, and the open squares indicate the 11 BL Lacs. The solid line is the regression line of all 50 blazars ($k = 1.15$, $r = 0.63$ and $p < 10^{-4}$), the dash line and dot line are the regression lines of FSRQs ($k = 1.12$, $r = 0.71$ and $p < 10^{-4}$) and BL Lacs ($k = 0.88$, $r = 0.68$ and $p = 2.2 \times 10^{-2}$), respectively.

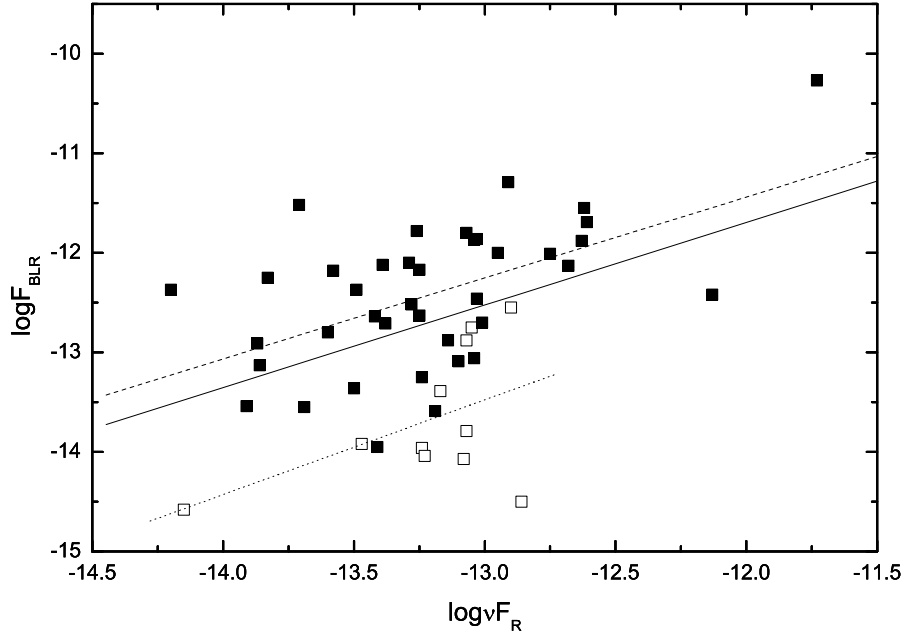


Fig. 4. Correlation between $\log \nu F_R$ and $\log F_{BLR}$ for 50 blazars. The filled squares indicate 39 FSRQs, and the open squares indicate the 11 BL Lacs. The solid line is the regression line of all 50 blazars ($k = 0.83$, $r = 0.43$ and $p = 1.9 \times 10^{-3}$), the dash line and dot line are the regression lines of FSRQs ($k = 0.81$, $r = 0.54$ and $p = 3.9 \times 10^{-4}$) and BL Lacs ($k = 0.95$, $r = 0.49$ and $p = 1.3 \times 10^{-1}$), respectively.

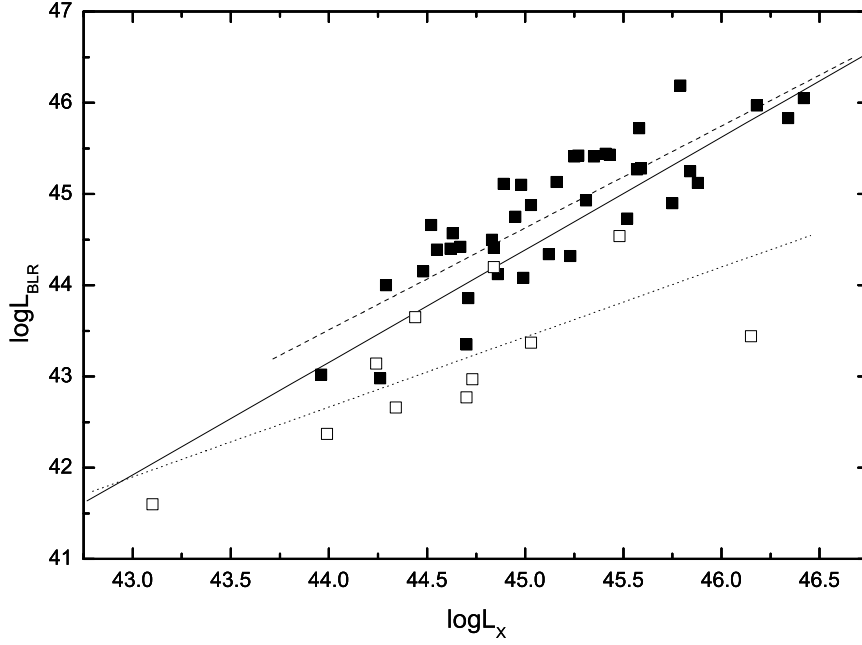


Fig. 5. Correlation between $\log L_X$ and $\log L_{BLR}$ for 50 blazars in high state. The filled squares indicate 39 FSRQs, and the open squares indicate the 11 BL Lacs. The solid line is the regression line of all 50 blazars ($k = 1.23$, $r = 0.78$ and $p < 10^{-4}$), the dash line and dot line are the regression lines of FSRQs ($k = 1.12$, $r = 0.84$ and $p < 10^{-4}$) and BL Lacs ($k = 0.77$, $r = 0.73$ and $p = 1.0 \times 10^{-2}$), respectively.

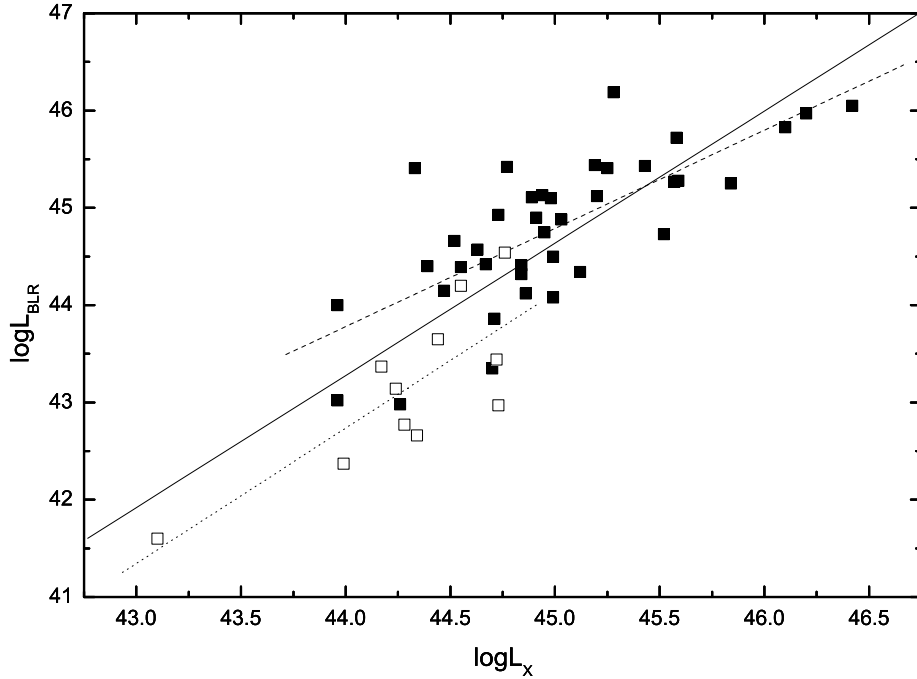


Fig. 6. Correlation between $\log L_X$ and $\log L_{BLR}$ for 50 blazars in low state. The filled squares indicate 39 FSRQs, and the open squares indicate the 11 BL Lacs. The solid line is the regression line of all 50 blazars ($k = 1.36$, $r = 0.81$ and $p < 10^{-4}$), the dash line and dot line are the regression lines of FSRQs ($k = 1.01$, $r = 0.74$ and $p < 10^{-4}$) and BL Lacs ($k = 1.39$, $r = 0.79$ and $p = 3.8 \times 10^{-3}$), respectively.

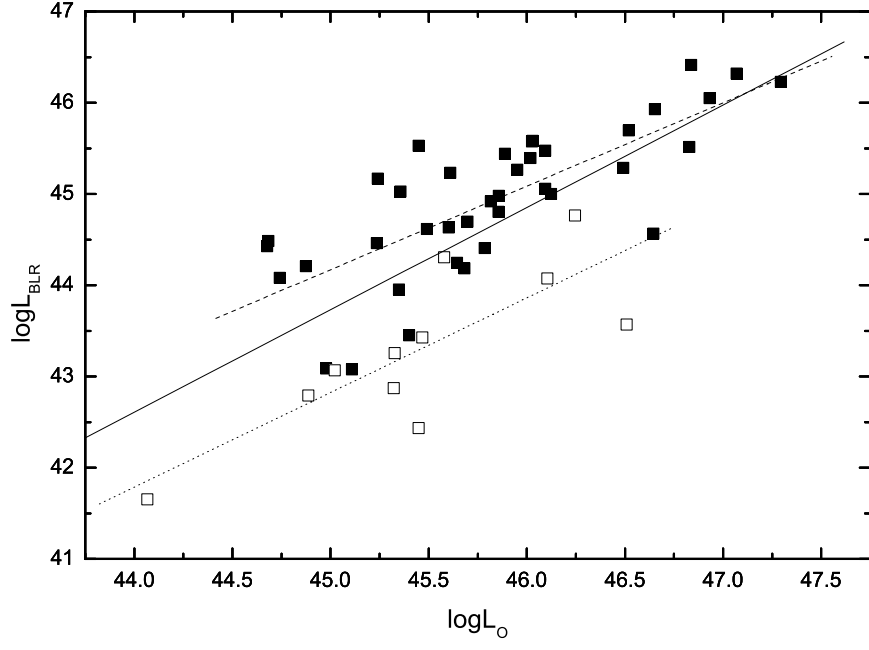


Fig. 7. Correlation between $\log L_O$ and $\log L_{BLR}$ for 50 blazars. The filled squares indicate 39 FSRQs, and the open squares indicate the 11 BL Lacs. The solid line is the regression line of all 50 blazars ($k = 1.12$, $r = 0.72$ and $p < 10^{-4}$), the dash line and dot line are the regression lines of FSRQs ($k = 0.92$, $r = 0.76$ and $p < 10^{-4}$) and BL Lacs ($k = 1.04$, $r = 0.80$ and $p = 3.1 \times 10^{-3}$), respectively.

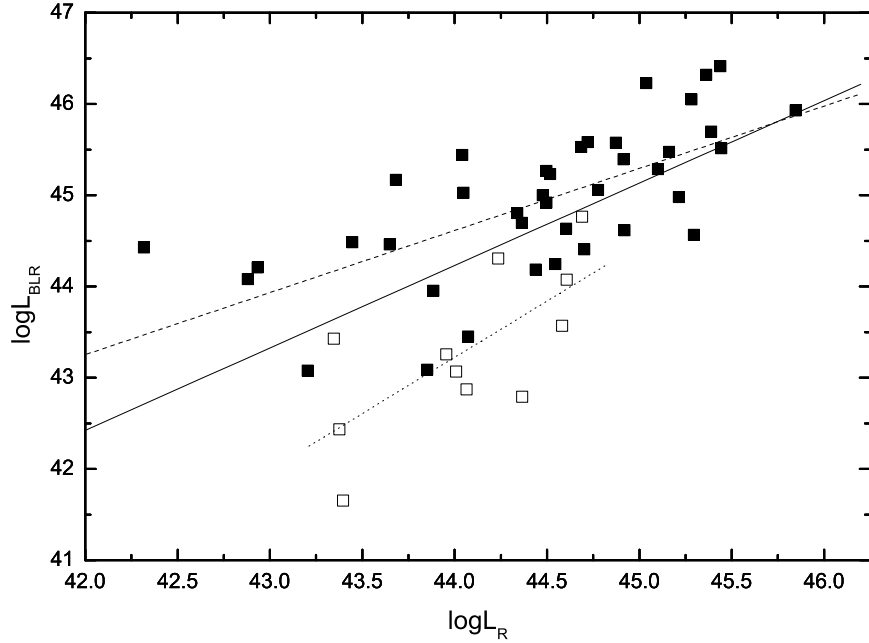


Fig. 8. Correlation between $\log L_R$ and $\log L_{BLR}$ for 50 blazars. The filled squares indicate 39 FSRQs, and the open squares indicate the 11 BL Lacs. The solid line is the regression line of all 50 blazars ($k = 0.90$, $r = 0.64$ and $p < 10^{-4}$), the dash line and dot line are the regression lines of FSRQs ($k = 0.68$, $r = 0.67$ and $p < 10^{-4}$) and BL Lacs ($k = 1.04$, $r = 0.70$ and $p = 1.6 \times 10^{-2}$), respectively.

Table 1. Sample of 50 Blazars and the Relevant Data. Q: quasars; BL: BL Lac objects.

IAU Name	z	F_R (Jy)	F_O (mJy)	F_X (μ Jy)	α	$\log F_{BLR}$ ($\text{erg cm}^{-2}\text{s}^{-1}$)	Class
0014+813	3.366	0.551	0.91	0.43	0.72	-12.37	Q
				0.35	0.89		
0016+731	1.781	1.750	0.06	0.05	0.43	-13.36	Q
0112-017	1.365	1.200	0.23	0.15	0.57	-12.80	Q
0133+476	0.859	2.920	0.47	0.30	0.92	-13.09	Q
0212+735	2.370	2.198	0.45	0.26	-0.34	-13.69	Q
0235+164	0.940	3.336	2.58	1.51	2.25	-13.79	BL
				0.15	0.75		
0237-233	2.223	3.520	0.81	0.39	0.68	-11.78	Q
				0.31	0.62		
0403-132	0.571	2.889	0.54	0.49	3.30	-11.86	Q
				0.40	0.78		
0420-014	0.915	3.720	0.34	0.37	-0.15	-12.70	Q
				0.28	0.85		
0537-286	3.104	0.990	0.04	0.18	0.36	-13.54	Q
				0.17	0.50		
0537-441	0.896	4.755	1.57	0.78	1.04	-12.55	BL
				0.17	0.27		
0637-752	0.651	5.849	2.38	3.76	0.45	-12.01	Q
				0.49	0.64		
0642+449	3.400	1.204	0.15	0.12	0.41	-12.91	Q
0736+017	0.191	1.999	1.33	1.49	1.82	-11.80	Q
				0.37	3.20		
0804+499	1.433	2.050	0.39	0.17	0.56	-12.71	Q
0814+425	0.258	3.500	0.15	0.05	0.16	-14.50	BL
0820+225	0.951	1.977	0.06	0.05	1.05	-14.58	BL
0836+710	2.170	2.590	1.06	2.26	0.31	-12.12	Q
				1.27	0.32		
0851+202	0.306	2.173	2.64	2.24	1.37	-12.88	BL
				0.37	0.71		
0906+430	0.670	1.300	0.16	0.11	0.57	-13.95	Q
0923+392	0.699	8.101	0.43	0.88	0.88	-11.55	Q
				0.37	0.36		
0945+408	1.252	1.450	0.38	0.11	0.96	-12.37	Q

Table 1. (Continued.)

IAU Name	z	F_R (Jy)	F_O (mJy)	F_X (μ Jy)	α	$\log F_{BLR}$ (erg cm $^{-2}$ s $^{-1}$)	Class
0954+556	0.909	2.169	0.43	0.10	1.17	-12.63	Q
0954+658	0.367	1.589	1.72	0.16	0.96	-14.04	BL
1034-293	0.312	1.510	1.11	0.24	0.41	-13.25	Q
1040+123	1.029	1.560	0.47	0.1	0.45	-12.64	Q
1055+018	0.888	3.470	0.40	0.21	0.93	-13.06	Q
1144-379	1.048	2.779	0.80	0.41	1.54	-13.39	BL
				0.14	0.70		
1150+497	0.334	0.699	0.560	0.63	0.77	-12.18	Q
				0.55	1.14		
1226+023	0.158	42.861	27.64	20.42	0.51	-10.27	Q
				1.96	0.57		
1253-055	0.536	14.950	1.66	1.50	0.65	-12.42	Q
				0.63	0.55		
1334-127	0.539	2.250	0.60	0.45	0.63	-12.88	Q
1442+101	3.530	1.260	0.28	0.12	1	-13.13	Q
1510-089	0.361	3.080	1.09	0.83	0.38	-12.00	Q
				0.49	0.35		
1538+149	0.605	2.648	0.44	0.28	1.13	-14.07	BL
				0.09	1.05		
1546+027	0.413	1.450	0.23	0.84	1.18	-12.10	Q
1611+343	1.404	2.671	0.35	0.24	0.76	-12.17	Q
1633+382	1.814	2.929	0.23	0.42	0.53	-12.52	Q
				0.25	0.51		
1641+399	0.594	7.821	0.89	0.98	0.85	-11.69	Q
				0.70	0.43		
1721+343	0.206	0.468	0.98	1.99	0.50	-11.52	Q
1803+784	0.684	3.016	0.61	0.26	1.42	-12.75	BL
				0.22	0.45		
1823+568	0.664	1.905	0.18	0.41	0.15	-13.96	BL
				0.27	0.96		
1928+738	0.360	3.339	1.11	1.47	1.33	-11.29	Q
				0.52	1.25		
2126-158	3.268	1.240	0.58	0.86	0.68	-12.25	Q
				0.71	2.18		
2134+004	1.936	12.249	0.72	0.26	0.82	-12.13	Q

Table 1. (Continued.)

IAU Name	z	F_R (Jy)	F_O (mJy)	F_X (μ Jy)	α	$\log F_{BLR}$ (erg cm $^{-2}$ s $^{-1}$)	Class
2155-152	0.672	2.150	0.42	0.22	1.17	-13.59	Q
2223-052	1.404	4.519	1.02	1.46	0.34	-12.46	Q
				0.22	0.73		
2230+114	1.037	3.689	0.69	0.73	0.51	-11.87	Q
				0.42	0.58		
2240-260	0.774	1.203	0.26	0.07	0.79	-13.92	BL
2251+158	0.859	8.759	1.02	1.37	0.62	-11.88	Q
				1.31	0.83		

Table 2. Linear Regression Analysis.

X	Y	N	A_0	k	r	p	class type
$\log \nu F_X$	$\log F_{BLR}$	50	-0.83	0.98	0.64	$< 10^{-4}$	Blazars
	(high state)						
$\log F_X$	$\log F_{BLR}$	39	-0.43	1.00	0.76	$< 10^{-4}$	FSRQ
	(high state)						
$\log \nu F_X$	$\log F_{BLR}$	11	-4.59	0.74	0.65	3.1×10^{-2}	BL Lac
	(high state)						
$\log \nu F_X$	$\log F_{BLR}$	50	4.14	1.37	0.67	$< 10^{-4}$	Blazars
	(low state)						
$\log \nu F_X$	$\log F_{BLR}$	39	0.82	1.09	0.63	$< 10^{-4}$	FSRQ
	(low state)						
$\log \nu F_X$	$\log F_{BLR}$	11	3.99	1.41	0.72	1.2×10^{-2}	BL Lac
	(low state)						
$\log \nu F_O$	$\log F_{BLR}$	50	4.06	1.15	0.63	$< 10^{-4}$	Blazars
$\log \nu F_O$	$\log F_{BLR}$	39	3.89	1.12	0.71	$< 10^{-4}$	FSRQ
$\log \nu F_O$	$\log F_{BLR}$	11	-0.74	0.88	0.68	2.2×10^{-2}	BL Lac
$\log \nu F_R$	$\log F_{BLR}$	50	-1.72	0.83	0.43	1.9×10^{-3}	Blazars
$\log \nu F_R$	$\log F_{BLR}$	39	-1.69	0.81	0.54	3.9×10^{-4}	FSRQ
$\log \nu F_R$	$\log F_{BLR}$	11	-1.11	0.95	0.49	1.3×10^{-1}	BL Lac
$\log L_X$	$\log L_{BLR}$	50	-11.12	1.23	0.78	$< 10^{-4}$	Blazars
	(high state)						
$\log L_X$	$\log L_{BLR}$	39	-5.62	1.12	0.84	$< 10^{-4}$	FSRQ
	(high state)						
$\log L_X$	$\log L_{BLR}$	11	8.95	0.77	0.73	1.0×10^{-2}	BL Lac
	(high state)						
$\log L_X$	$\log L_{BLR}$	50	-16.51	1.36	0.81	$< 10^{-4}$	Blazars
	(low state)						
$\log L_X$	$\log L_{BLR}$	39	-0.62	1.01	0.74	$< 10^{-4}$	FSRQ
	(low state)						
$\log L_X$	$\log L_{BLR}$	11	-18.45	1.39	0.79	3.8×10^{-3}	BL Lac
	(low state)						
$\log L_O$	$\log L_{BLR}$	50	-6.78	1.12	0.72	$< 10^{-4}$	Blazars
$\log L_O$	$\log L_{BLR}$	39	3.02	0.92	0.76	$< 10^{-4}$	FSRQ
$\log L_O$	$\log L_{BLR}$	11	-3.83	1.04	0.80	3.1×10^{-3}	BL Lac
$\log L_R$	$\log L_{BLR}$	50	4.49	0.9	0.64	$< 10^{-4}$	Blazars
$\log L_R$	$\log L_{BLR}$	39	14.65	0.68	0.67	$< 10^{-4}$	FSRQ
$\log L_R$	$\log L_{BLR}$	11	-11.02	1.23	0.70	1.6×10^{-2}	BL Lac

Note: The linear regression is obtained by considering X to be the independent variable and assuming a relation $Y = kX + A_0$; N is the number of points, r is the correlation coefficient, and p is the chance probability.